Available online at www.sciencedirect.com
SCIENCE DIRECT®
Journal of Hydrology 287 (2004) 124–146
Journal of Hydrology
www.elsevier.com/locate/jhydrol

Hydrological consequences of landscape fragmentation in mountainous northern Vietnam: evidence of accelerated overland flow generation

Alan D. Ziegler[a,b,*], Thomas W. Giambelluca[a], Liem T. Tran[c], Thomas T. Vana[a], Michael A. Nullet[a], Jefferson Fox[d], Tran Duc Vien[e], Jitti Pinthong[f], J.F. Maxwell[g], Steve Evett[h]

[a]*Geography Department, University of Hawaii, 2424 Maile Way SSB 445, Honolulu, HI 96822, USA*
[b]*Geography Department, National University Singapore, 1 Arts Link, Kent Vale, Singapore*
[c]*Department of Geography & Geology, Florida Atlantic University, Boca Raton, FL, USA*
[d]*Environmental Studies Program, Jefferson Hall, East–West Center, Honolulu, HI 96848, USA*
[e]*Center for Natural Resources and Environmental Studies (CRES), Vietnam National University, Hanoi, Vietnam*
[f]*Soil Survey Division, Faculty of Agriculture, Chiang Mai University, Chiang Mai, Thailand*
[g]*Herbarium, Department of Biology, Faculty of Science, Chiang Mai University, Chiang Mai, Thailand*
[h]*USDA-ARS, 2300 Experiment Station Road, Bushland, TX 79012-0010, USA*

Received 7 January 2003; revised 1 July 2003; accepted 26 September 2003

Abstract

Measurements of saturated hydraulic conductivity (K_s) and indices of Horton overland flow (HOF) generation are used to assess the influence of landscape fragmentation on near-surface hydrologic response in two upland watersheds in northern Vietnam. The fragmented landscape, which results from timber extraction and swidden agriculture, is a mosaic of surfaces having distinct infiltration characteristics. In general, human activity has reduced infiltration and altered near-surface flow paths on all disturbed land covers. Compacted roads, paths, and dwelling sites, for example, have the propensity to generate HOF for small rainfall depths. Although these surfaces occupy a small fraction of a basin land area (estimated at $<1\%$), they contribute disproportionately to overland flow response during typical rainfall events. Recently abandoned fields have the lowest K_s of all non-consolidated, post-cultivation surfaces tested. Beginning 1–2 years following abandonment, diminished K_s recovers over time with the succession to more advanced types of secondary regrowth. If a grassland emerges on the abandoned site, rather than a bamboo-dominated cover, K_s recovers more rapidly. The decrease in K_s with depth below disturbed surfaces is more acute than that found at undisturbed sites. This enhanced anisotropy in near-surface K_s increases the likelihood of the development of a lateral subsurface flow component during large storms of the monsoon rain season. Subsequently, the likelihood of return flow generation is increased. Because the recovery time of subsurface K_s is greater than that for the surface K_s, the impact human activity has on hydrologic response in the fragmented basin may linger long after the surface vegetation has evolved to a mature forested association.

* Corresponding author. Address: Department of Geography, University of Hawaii, 2424 Maile Way, 445 Porteus Hall, Honolulu, HI 96822, USA. Fax: +808-956-3512.
E-mail address: adz@hawaii.edu (A.D. Ziegler).

0022-1694/$ - see front matter © 2003 Elsevier B.V. All rights reserved.
doi:10.1016/j.jhydrol.2003.09.027

Keywords: Land-cover change; Tropical watershed hydrology; Deforestation; SE Asia; Saturated hydraulic conductivity; Infiltration; Disk permeameter; *Imperata cylindrica*

1. Introduction

Vast forests in many upland watersheds of mainland SE Asia have now been replaced by fragmented landscapes consisting of remnant forest patches and various human-disturbed land covers. Fragmentation in the Da River Watershed of northern Vietnam results from myriad activities, including timber extraction, swidden/shifting agriculture, permanent cultivation, forest gathering, dwelling construction, road building, and in some cases, revegetation (cf. Cuc and Rambo, 1999; Fox et al., 2001). Shifting agriculture and timber removal are cited commonly as major causes of watershed degradation (e.g. soil and nutrient loss) and associated downstream environmental impacts (e.g. reservoir sedimentation, floods/droughts) in the uplands of Vietnam (Sharma, 1992; Tuan, 1993). As much as 1.5–3.5 million ha may currently be utilized for shifting agriculture by the members of about 50 ethnic groups who live in the highlands of Vietnam (Vien, 1997). Forested land is reported to have declined from 14.4 million ha in the early 1940s to 7.8 million ha in the early 1980s (Thai and Nguyen, 1992). Today, only about 3 million ha of dense forest remain (Van Bo et al., 2001). A 1990 survey by the Vietnamese Ministry of Forestry reported that 100,000 ha of forest are 'lost' annually. As much as 50% of this loss may be related to shifting cultivation alone (unpublished report cited by Vien, 1997). Fox et al. (2000) point out that many national governments in SE Asia are prone to blame shifting cultivators for the rapid forest loss that has occurred in the past 20 years (Do Van, 1994; Cuc, 1996; Rambo, 1996). Furthermore, they state that such blame may be unjustified—as shown by Nguyen and van der Poel (1993), who found no correlation between the occurrence of shifting agriculture and deforestation. Regardless of the cause of forest removal, compared with the continuous tracts of old-growth forest that once predominated this region, the fragmented landscapes now commonly in existence are degraded both ecologically and physically.

The realm of hydrological consequences associated with fragmentation is not understood clearly. Forest removal in general produces a wide range of hydrological responses (Hibbert, 1967; Dunne and Leopold, 1978; Bosch and Hewlett, 1982; Bruijnzeel, 2000). One of the most common is an increase in runoff, with proportional increases varying from one basin to another (Jones, 1997). Alteration of runoff response is accomplished, in part, through disruption of typical hydrological pathways through which storm water moves to the stream. One critical disruption is an increase in overland flow. For example, we found evidence of accelerated overland flow generation in a disturbed upland watershed in northern Thailand. Data from rainfall simulation experiments and saturated hydraulic conductivity (K_s) measurements show convincingly that the various land covers comprising the fragmented landscape differ in their capability to infiltrate rainwater (Ziegler and Giambelluca, 1997; Ziegler et al., 2000). Human-disturbed surfaces having low K_s, such as roads and footpaths, act as source areas for Horton overland flow (HOF, rainfall rate in excess of infiltration rate and surface storage; Horton, 1933). In contrast, K_s on densely vegetated surfaces is typically sufficient to allow infiltration of relatively high-intensity rainfall. Other disturbed, vegetated land covers having intermediate values of K_s are potential sources for HOF during large rainfall events.

In general, overland flow can also result from mechanisms other than HOF (cf. Kirkby, 1988). Saturation overland flow, for example, is produced when the storage capacity of the soil is exceeded (e.g. saturation via a rising water table) and subsequent additions of rain water flow across the surface (Dunne and Black, 1970); and return flow (RF) occurs when subsurface flow resurges on the surface (Cook, 1946; Hewlett and Hibbert, 1967). With respect to fragmentation, if the collective processes that disturbed the landscape produce flow-restricting layers within the near-surface soil profile, hillslope overland flow may then be augmented by the addition of RF during some storms (dependent

on storm characteristics, antecedent moisture conditions, vegetation, and topography).

In this study, we investigate overland flow generation in two fragmented basins in northern Vietnam. Herein we (1) quantify surface K_s for the dominant land-cover groups; (2) determine the propensity of each land cover to produce overland flow; (3) explore the possible effects of land-cover conversion on the near-surface hydrological pathways that influence subsurface flow. In a related work, ('Hydrological Consequences of Landscape Fragmentation in Mountainous Northern Vietnam: Buffering of Accelerated Overland Flow', submitted to *Hydrological Processes,* referred to hereafter as 'Ziegler et al., submitted paper') we address buffering/filtering of overland flow in the same fragmented study area.

2. Study area

Field measurements were conducted in Tanh Minh Village (roughly 19:00N, 104:45E), which is located SSW of Hanoi, in Da Bac District of Hoa Binh Province, northern Vietnam (Fig. 1). Field measurements were performed within the general vicinity of Tat, one of 10 hamlets comprising Tanh Minh. The site is within the Da (Black) River Watershed, in a region characterized by sinuous narrow valleys and steep mountains. The elevation of Tanh Minh is approximately 360 m a.s.l.; surrounding mountain peaks rise to 800–950 m a.s.l. The highest peaks in the region extend to 3000 m a.s.l. (e.g. Fan Si Fan, Ta Giang Phing). The topography is steep: 30–60° slopes typically extend down to the valley floor and/or stream channel.

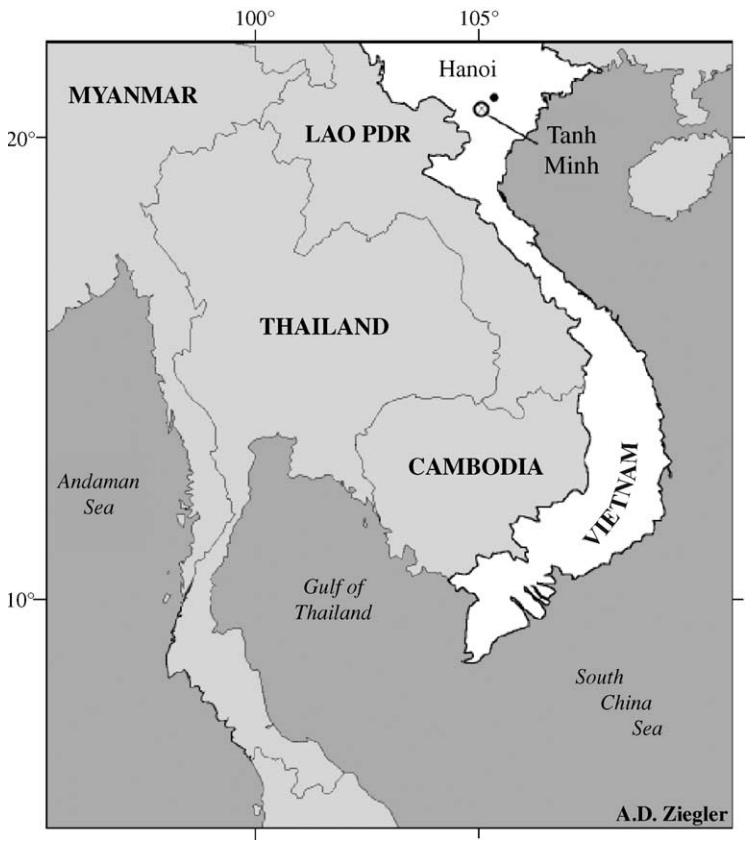

Fig. 1. (a) The field site, Tanh Minh, located SW of Hanoi in Hoa Binh Province of northern Vietnam.

Only 20% of the area has a slope $<25°$. The narrow valley floor is typically the only part of the landscape flat enough for permanent settlement and paddy rice cultivation. Parent bedrock is largely sandstone and schist, with some quartz and mica-bearing granite present. Soils are pre-dominantly Ultisols of the Udic moisture regime, viz. Hapludults and Kandiudults (i.e. low-activity clays in the B horizons), with some Paleudults and Kanhapludults as inclusion. The general soil texture class is sandy clay loam (USDA, 1993); measured sand, silt, and clay fractions are 45, 26, and 29%, respectively.

The climate is characterized as tropical monsoon, with approximately 90% of an annual 1800 mm of rainfall occurring between May and October. Much of the area around Tanh Minh remained forested until the 1950s (Fox et al., 2001). Today, remnant forest patches exist primarily on steep, inaccessible peaks, runs, and slopes (Fig. 2b and d). Some accessible ridgelines do,

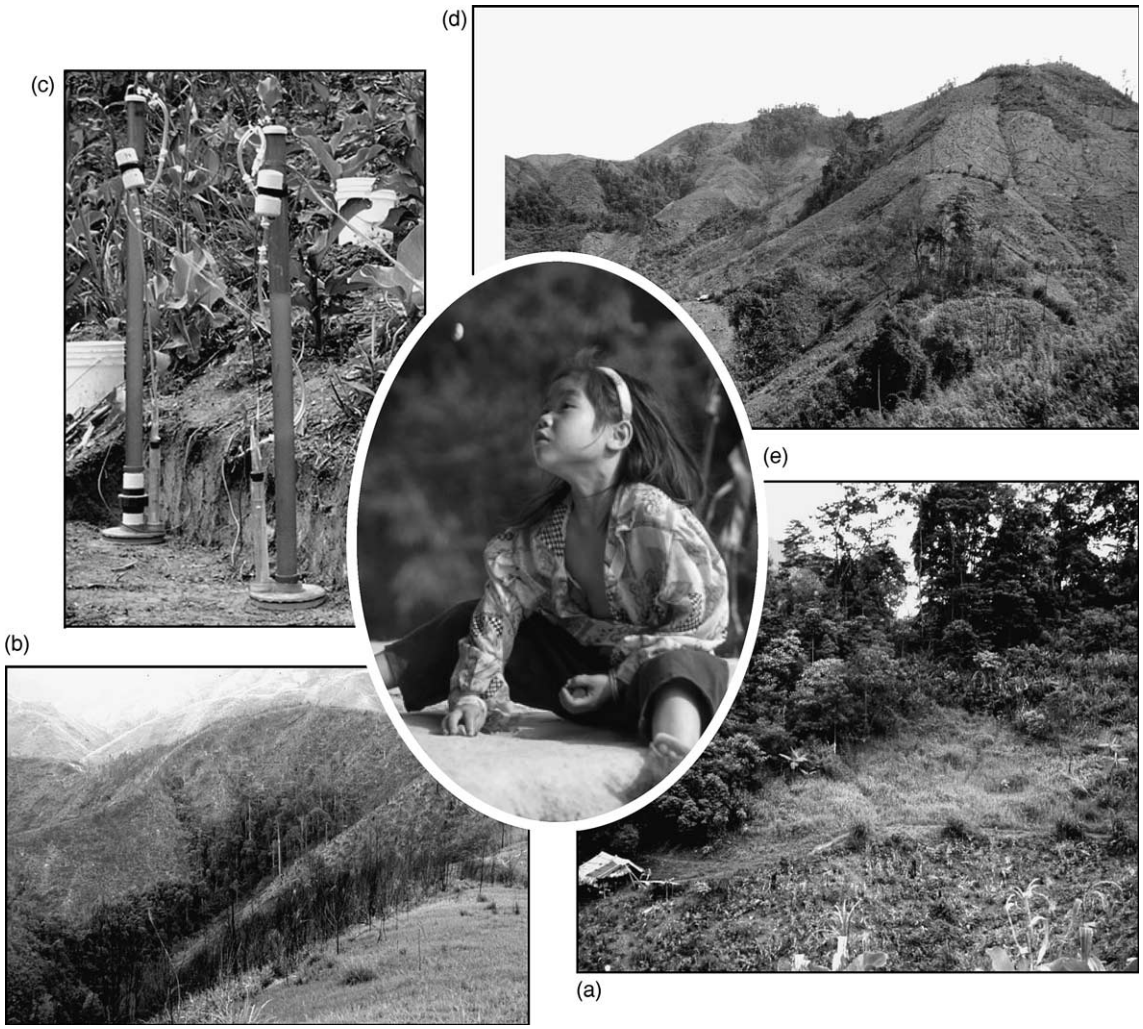

Fig. 2. (a) A representative mosaic of fragmented surfaces, including forest, secondary vegetation (young and intermediate), grassland, swidden fields (both active and in fallow), and a compacted access path; (b) A forest fragment, located within a steep, practically inaccessible hollow; (c) Disk permeameters measuring infiltration at a subsurface depth of 0.4 m on an active field; (d) Typical cleared hillslope, playing host to forest fragments, an assortment of active/abandoned swidden fields, and secondary vegetation; (e) A Tay child at play.

however, host mature secondary forests. Mountain slopes are dotted with active swidden fields that are farmed by the Tay villagers, the principal inhabitants of Tanh Minh (Fig. 2e). Juxtaposed with the active fields are recently abandoned fields and lands in various stages of secondary regrowth (i.e. mixtures of grasses, herbs, bamboo, and trees) on former cultivated sites (Fig. 2a). The farming system and other physical aspects are described elsewhere (Rambo, 1996; Cuc and Rambo, 1999; Fox et al., 2000).

3. Methods

3.1. Saturated hydraulic conductivity (K_s) measurements

We focus on K_s because it is a key property in the activation of flowpaths in almost all modes of streamflow generation (Elsenbeer and Lack, 1996; Elsenbeer, 2001). While the influence of K_s at the soil surface on the production of HOF is intuitive, depth-related differences in K_s (Zavslavsky and Rogowski, 1969) can contribute to the generation of RF. A simplified example is water moving 'laterally' as subsurface flow above a restricting soil layer until it exits the surface at some downslope location, which may be related to topographical characteristics such as slope concavity. Herein, we examine spatial patterns in both surface (i.e. the mineral layer immediately below leaf debris) and subsurface (down to 0.7 m) K_s to determine if the likelihood of overland flow generation is different now than it was before disturbance.

We measured K_s during two field campaigns conducted between March and June, 1998. All non-consolidated K_s sites are located within two relatively small areas, located on the hillslope and ridgeline immediately above Tanh Minh (referred to as Có Hiân and Có Nôm, Fig. 3a). Most measurements were collected in Có Hiân between meteorological sites 301 and 304 (Fig. 3c); the measurements on abandoned fields were collected in Có Nôm. The meteorological network is discussed elsewhere (Giambelluca et al., 2003). Near each of the four meteorological stations in Có Hiân, we conducted the subsurface K_s measurements at depths of 0.1, 0.4, and 0.7 m (Fig. 2c).

Saturated hydraulic conductivity is estimated from infiltration measurements taken in situ with a Vadose Zone Equipment Corporation (Amarillo, TX) disk permeameter, operated at zero tension. The constant head permeameter is fitted with a pressure transducer; and data are recorded with a Campbell (Logan, UT) 21× logger. The permeameter is a modification of the design described by Perroux and White (1988). In general, we chose flat measurement sites to avoid excavating the soil surface (subsurface measurements sites were excavated with a shovel). We cut roots, rather than pulling them, to avoid creation of artificial macropores. Similarly, we avoided sites with visible macropores. We used fine sand as a contact medium between the soil surface and the permeameter base (20–40 μm nylon mesh membrane). To improve contact between the sand and membrane, we employed some of the procedures discussed by Close et al. (1998): e.g. soaking the membrane base for 12 h before use; and rotating the permeameter clockwise/counterclockwise when placing it on the sand medium. We used a metal retention ring to apply an even sand layer on the measurement location, but typically removed the ring before placing the permeameter on the sand, thereby allowing the membrane base to mold to the sand surface.

Our K_s calculation methodology is akin to the "Short- and Long-Time Observations" with disc permeameters described by Clothier (2000). Briefly, we conducted measurements until a steady state infiltration rate was detected or until all water had been drained from the permeameter reservoir (measurement duration lasted anywhere from 15 to 120 min). Values of K_s [LT^{-1}] were calculated following White (1988)

$$K_s = I - \frac{4bS^2}{\pi r(\Theta_0 - \Theta_n)} \quad (1)$$

where Θ_n is volumetric moisture content of the 'dry' in situ soil, determined from a bulk density sample collected before K_s measurement (90 cm^3 core collected from the upper 5-cm of soil and oven dried at 105 °C for 24 h); Θ_0, volumetric moisture content of the 'wet' in situ soil, calculated from a grab sample collected from the upper 1 cm of soil below the sand contact medium immediately after measurement (Θ_0 is then calculated using the bulk

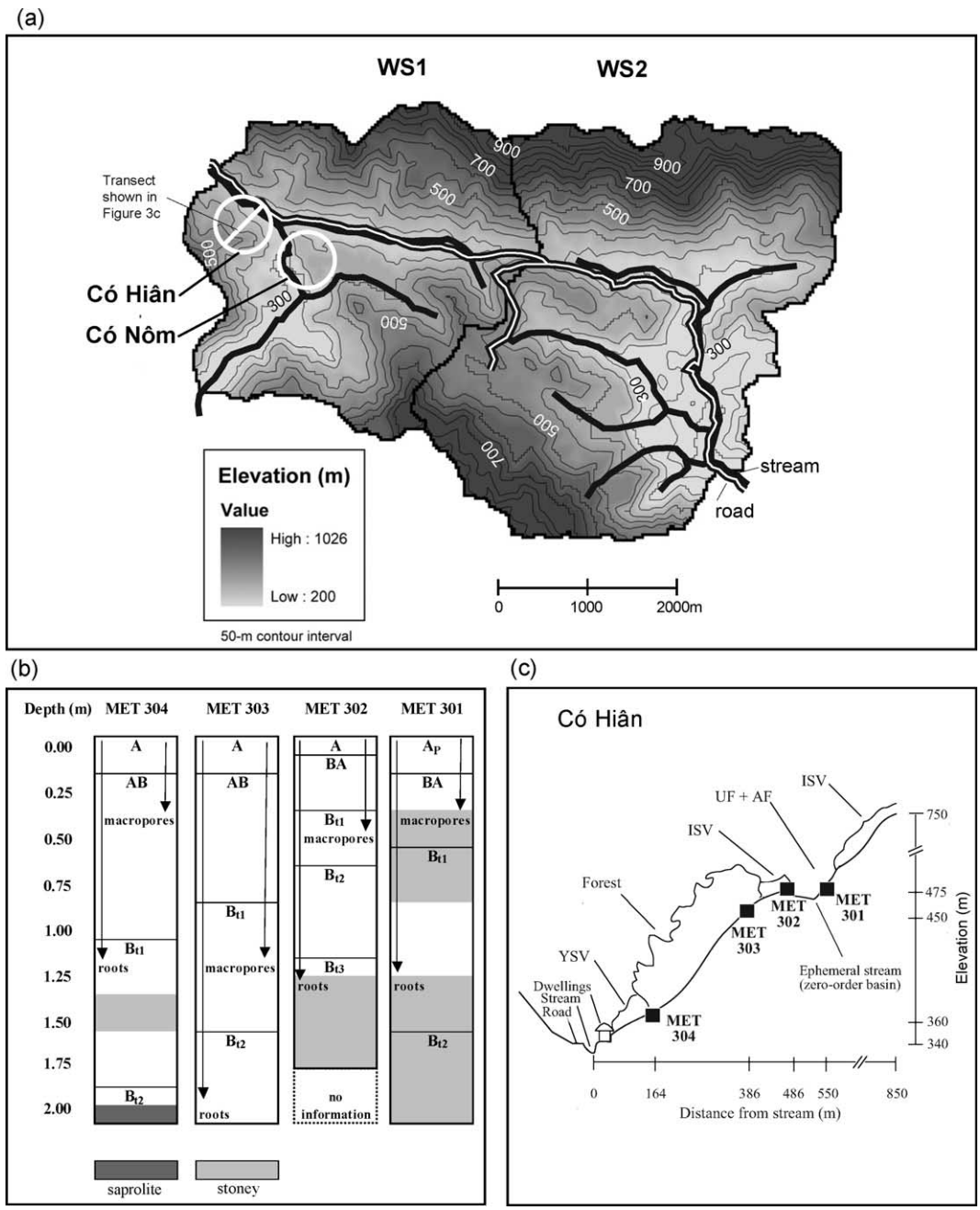

Fig. 3. (a) Elevation map of the two watersheds (WS1 and WS2) comprising the Tanh Minh study area. Shown are the two locations where K_s measurements were taken (Có Hiân and Có Nôm). Note the proximity of the road (double line) to the stream (solid line). (b) Characterization of four soil profiles where subsurface K_s measurements were taken. The location names, which refer to meteorological stations discussed in another work (Giambelluca et al., 2003), correspond to those on the transect in panel c. Horizon descriptions (A_p, A, AB, BA, B_{t1-3}) are based on observed profiles; AB and BA represent transitional horizons for which the ordering reflects the resemblance to either the A or B horizon; *p* signifies a 'plow' layer; and t refers to the presence of clay (cf. USDA, 1993). (c) A profile of the hillslope in Có Hiân showing the general location where the K_s and other soil information was obtained; the profile location is indicated in panel a.

density determined from the cored sample); r, the radius of the disk permeameter base (0.1 m); b, the constant 0.55, which is the estimate of the hydraulic conductivity corresponding to soil water pressure head applied by the disk (provided by the manufacturer); S, the sorptivity obtained by plotting cumulative infiltration versus the square root of time at the start of infiltration, after the pore space in the sand layer had been filled; I is the infiltration rate, calculated as

$$I = \frac{q}{\pi r^2} \tag{2}$$

where q is the slope of the plot of cumulative flow (from the permeameter into the soil) versus time, after the flow rate has reached a steady state; and r is as above.

Saturated hydraulic conductivity data typically do not follow a normal distribution—in some cases, K_s data have been shown to be lognormally distributed (cf. Rogowski, 1972; Nielsen et al., 1973). A preliminary analysis of our data using the techniques discussed by Elsenbeer et al. (1992) highlighted their non-Gaussian behavior. We therefore used a non-parametric approach that makes use of (1) detailed box plots (Tukey, 1977; McGill et al., 1978) as the data summary, (2) the median as the estimator of central tendency, (3) the median absolute deviation (MAD) as the estimator of scale, (4) 95% confidence intervals about the median. The MAD is computed as

$$\text{MAD} = \text{median}|x_i - M|, \qquad \text{for } i = 1, 2, \ldots, n \tag{3}$$

where M is the median of n values of x.

3.2. Rainfall and HOF indices

One-minute rainfall intensity (I_1) values were recorded from 26 March to 29 June 1998 with a MET-ONE (Grants Pass, OR) tipping bucket rain gauge and Campbell logger. This period encompasses the transition from the dry to rainy season. During low intensity periods, rainfall can accumulate for more than one min in the 0.254-mm tipping bucket before being recorded as 'one-tip' by the logger. We correct for this by distributing the first 0.254 mm depth, recorded following a rain-free period within an event, equally among each preceding minute. Note the initial value defining the beginning of an event was not corrected, because it is impossible to determine when the rainfall began.

Storm events were defined initially using the criteria of Wischmeier and Smith (1978): a storm is an event that accumulates at least 12.7 mm without a 6-h rain-free period, or an event having at least 6.4 mm within any 15-min period. As a slight modification, we do not allow a storm to have a rain-free period longer than 4 h, unless more than half of the total rainfall depth occurs following the gap. We use these criteria simply to demarcate storms in the composite rainfall data set. They may or may not be more appropriate than other criteria for delineating storms in tropical regions, e.g. Hudson's (1971) characterization of 'erosive events'. As an index of relative storm size, we rank the events by maximum 30-min rainfall intensity (I_{30_MAX}); I_{1_MAX}, I_{10_MAX}, I_{20_MAX}, and I_{60_MAX} refer to maximum 1-, 10-, 20-, and 60-min rainfall intensities.

3.3. Simulating HOF generation

To help answer questions regarding the propensity of each land cover to generate HOF, we conduct a suite of diagnostic computer simulations using the KINEROS2 runoff model (Smith et al., 1995, 1999). The simulations look simply at the influence of soil properties, vegetation characteristics, and rainfall phenomena on HOF generation on 30 m × 30 m plots of each major land cover during observed storms. The plot size corresponds to the area of one pixel in a LANDSAT image, which we use to determine the land-cover distribution.

KINEROS2 is an event-based, physics-based runoff and erosion model. Overland flow simulation in KINEROS2 utilizes the kinematic wave method to solve the dynamic water balance equation

$$\frac{\partial h}{\partial t} + \frac{\partial Q}{\partial x} = q(x,t) \tag{4}$$

where h is water storage per unit area; $Q(x,t)$, the water discharge; x, the distance downslope; t, the time; $q(x,t)$ is the net lateral inflow rate. Solution of Eq. (4) requires estimates of time- and space-dependent

Table 1
Parameters used for the KINEROS2 overland flow simulations

Land cover	K_s (mm h^{-1})	C_v (–)	Porosity (–)	n	Ca (–)	Int (mm)
Upland field, UF	103	0.39	0.57	0.05	0.10	0.50
Abandoned field, AF	28	0.36	0.57	0.13	0.50	0.25
Grassland, GL	93	0.31	0.57	0.24	0.90	2.00
Young secondary vegetation, YSV	32	0.47	0.63	0.20	0.75	1.65
Intermediate secondary vegetation, ISV	67	0.58	0.55	0.20	0.80	1.75
Forest, F	63	0.49	0.61	0.15	0.85	1.80
Consolidated surfaces, CS	7	0.36	0.40	0.02	0.05	0.05

Variables are saturated hydraulic conductivity (K_s), the coefficient of variation for K_s (C_v), Manning's n, vegetation coverage (Ca), total interception depth (Int). The following variables are the same for all land covers: capillary drive (82.58 mm), initial soil saturation index (SAT = 0.833, wet season value corresponding to saturation), slope (0.84 m m^{-1}), volumetric rock fraction (1%), particle density (2.49 g cm^{-3}), pore size distribution index (0.25), average microtopography relief and spacing (2 mm and 0.3 m, respectively). All values are based on field observations/measurements, except for capillary drive, which is adjusted during calibration (Ziegler et al., submitted manuscript). For all simulation surfaces, the soil class is sandy clay loam.

rainfall $r(x,t)$ and infiltration $f(x,t)$ rates:

$$q(x,t) = r(x,t) - f(x,t) \tag{5}$$

Infiltrability in KINEROS2 is defined as the limiting rate at which water can enter the soil surface (Hillel, 1971). Modeling of this process utilizes several input parameters describing the soil profile: inter alia, K_s, integral capillary drive or matric potential (G), porosity (ϕ), and pore size distribution index (Brooks and Corey, 1964); the coefficient of variation for K_s can also be specified to account for spatial variation. The general infiltrability (f_c) equation is a function of cumulative infiltrated depth (I), following Parlange et al. (1982)

$$f_c = K_s\left[1 + \frac{a}{e^{(aI/B)} - 1}\right] \tag{6}$$

where a is a parameter related to soil type (fixed in most applications at 0.85); and $B = (G + h_w) \times (\Theta_s - \Theta_i)$, for which G is as above, h_w is surface water depth (computed during simulation); and the second term, unit storage capacity, is the difference of maximum (Θ_s) and initial (Θ_i) soil moisture contents. Antecedent soil moisture conditions for each storm are parameterized in KINEROS2 by assigning a value for the initial soil saturation index (SAT). Hillslopes in KINEROS2 are treated as a cascading network of surface and channel elements. Each element is characterized by assigning values to parameters that determine the event infiltration rate, and therefore, runoff generation.

Prior to simulation, we calibrated KINEROS2 using rainfall simulation data obtained from small-scale (≈ 3 m^2) plot experiments on an abandoned upland rice field in northern Thailand (Ziegler et al., 2001). Resulting total error, error in the peak estimate, and root mean squared error for the KINEROS2 overland flow predictions of the simulation data were acceptably low: <1, 5, and 16%, respectively. The abandoned field in Thailand is similar to those in Tanh Minh in terms of vegetation characteristics (e.g. coverage, height, interception, age since usage). The diagnostic overland flow simulations are performed by replacing KINEROS2 parameters used in the Thailand calibration simulations with those obtained from field measurements in Vietnam (e.g. K_s, slope, saturation, interception, percent cover, and porosity). Parameter values used for each simulation surface are listed in Table 1. Calibration of KINEROS2 is discussed further by Ziegler et al. (submitted paper).

4. Results

4.1. Dominant land-cover groups

Land-cover distribution in Tanh Minh is derived from the supervised classification of a LANDSAT

Thematic Mapper multispectral image (7 November 1998), using the maximum likelihood classification scheme in the ERDAS *Imagine* geographical information system (GIS). Classification and ground truthing (described by Fox et al. (2000)) reveal that the Tanh Minh landscape is a mosaic of upland fields (cultivated, slashed, abandoned/fallow), various stages of secondary regrowth (including reemerging trees mixed with stands of bamboo and under-story vegetation, grasslands, and shrublands), forest (of various stages of disturbance), and consolidated surfaces (paths, roads, hut complexes). Based on vegetation structure and age since abandonment of cultivation, we distinguish eight major land covers: upland fields (UF), abandoned fields (AF), young secondary vegetation (YSV), grassland (GL), intermediate secondary vegetation (ISV), forest (F; note, we do not distinguish between primary and secondary forest), consolidated surfaces (CS), and paddy fields. Table 2 provides vegetation descriptions for the six land covers found commonly on the hillslopes.

Fig. 4 shows the land-cover distribution in the two studied watersheds; every pixel represents a 30 m × 30 m area on the ground. Table 3 lists for the various land covers the following statistics: (1) total area coverage (ha), (2) percent cover, (3) total number of patches, and (4) mean patch area (ha). Grasslands occupy the largest area in the combined watersheds (38%) and have the largest mean patch area (13.7 ha per patch; 59 patches). The abandoned field land cover is composed of the greatest number of individual patches (149); and UF has the second most number of patches (104). Together these two types of agricultural surfaces comprise 30% of the total area in Tanh Minh. Note that Table 3 includes rice paddies, which are not studied in detail in this paper (discussed below). Consolidated surfaces are not included in Table 3 because they were not distinguished in the LANDSAT classification, as they are subpixel phenomena. We estimate the areal extent of CS to be less than 1% in Tanh Minh.

4.2. Surface K_s

Descriptive statistics for K_s and bulk density are listed in Table 4. Median K_s on consolidated surfaces, including roads, footpaths, and dwelling sites is 1–2 orders of magnitude lower than all other surfaces (7 mm h^{-1}). Upland field and forest have large ranges in K_s values (roughly 20–330 and 10–290 mm h^{-1}, respectively). Fig. 5 shows box plots of the K_s data for the seven land covers considered. Statistical features are explained in the inset. Based on visual inspection of the 95% confidence intervals and medians, we recognize the following groupings: {upland field, grasslands} > {abandoned field, young secondary vegetation} > {consolidated surfaces}, with forest and intermediate secondary vegetation being indistinguishable from the first two groups.

In Fig. 6, surface K_s is presented with box widths bracketing (1) the approximate age when the land cover appears on the landscape with respect to abandonment of a swidden site and (2) the approximate age when it gives way to a more advanced land cover. A dramatic reduction in K_s begins following abandonment: median K_s decreases from >100 mm h^{-1} on UF to <30 mm h^{-1} on AF. The pattern of recovery in K_s is then dependent on the type of land cover that replaces AF, i.e. YSV versus GL. Median K_s on the YSV class is only slightly higher than that for abandoned field (32 versus 28 mm h^{-1}). In contrast, GL has a higher median K_s value (>90 mm h^{-1}).

4.3. Storm rainfall intensity and HOF indices

Of a total of 49 rainfall events recorded during the collection period, only 11 were classified as storms using the criteria explained in Section 3.2. Event duration, total rainfall, average rainfall (I_{event}), and maximum 1-, 10-, 20-, 30-, and 60-min intensities for these storms are listed in Table 5. The 11 storms are ranked in descending order from largest to smallest, as indicated by the I_{30_MAX} data. Table 6 lists the total number of one-min intensity values (I_1) during each of the 11 storms that are greater than median K_s on the seven land covers considered. Periods where I_1 exceeds K_s represent periods when HOF generation is possible, especially if this magnitude of rainfall intensity is sustained long enough for ponding to be overcome. Data regarding sustained rainfall intensity are presented as I_{10_MAX}, I_{20_MAX}, I_{30_MAX}, and I_{60_MAX} values in Table 5.

Table 2
Vegetation characteristics of the major hillslope land covers in Tanh Minh

Land cover	ID	Description
Upland field	UF	Active swidden fields, including corn (*Zea mays* L. (Gramineae), banana (*Musa coccinea* Andr. (Musaceae), *Musa paradisiacal* L. (Musaceae)), and canna (*Canna edulis* Ker (Cannacea)). Weedy volunteer vegetation include *Ageratum conyzoides* L. (Compositae), *Eupatorium odoratum* L. (Compositae), *Euphorbia hirta* L. (Euphorbiaceae), *Crassocephalum crepidioides* (Bth.) S. Moore (Compositae), *Imperata cylindrica* (L.) P. Beauv. var. *major* (Nees) C.E. Hubb. *ex* Hubb. & Vaugh. (Gramineae), *Melia aderazach* L. (Meliaceae), *Rorippa indica* (L.) Hiern (Cruciferae), *Saccharum spontaneum* L. (Gramineae), *Setaria palmifolia* (Korn.) Stapf var. *palmifolia* (Gramineae), *Solanum verbascifolium* L. (Solanaceae), and *Urena lobata* L. ssp. *lobata* var. *lobata* (Malvaceae). Bare ground is approximately 30–50%.
Abandoned field	AF	Short grasses, herbs, and shrubs occurring on abandoned fields or lands where grazing may prevent tall vegetation from occurring. Species include *Helicteres angustifolia* L (Sterculiaceae), *Imperata cylindrica*, *Microstegium vagans* (Nees *ex* Steud.) A. Camus (Gramineae), *Miscanthus japonicus* (Thunb.) And. (Gramineae), *Paspalum conjugatum* Beerg. (Gramineae), *Rorippa indica*, *Saccharum spontaneum*, *Litsea cubeba* (Lour.) Pers. var. *cubeba* (Lauraceae), and *Mallotus albus* M.-A. (Euphorbiaceae).
Young secondary vegetation	YSV	Evergreen broadleaf bush mixed with **nua** (*Neohouzeoua dullooa* (Gamb.) A. Camus (Gramineae, Bambusoideae)) bamboo occurring in areas where forest was once cleared. Representative species include *Acacia pennata* (L.) Willd. (Leguminosae, Mimosoideae), *Cyperus nutans* Vahl (Cyperaceae), *Rauvolfia cambodiana* Pierre *ex* Pit. (Apocynaceae), *Eupatorium odoratum*, *Ficus* sp. (Moraceae), *Microstegium vagans*, *Saccharum spontaneum*, and *Urena lobata*.
Grassland	GL	Tall grasslands occurring where forest has been cleared and, perhaps, the land overworked during farming. Three species dominating this land cover, *Imperata cylindrica*, *Thysanolaena latifolia* (Roxb. *ex* Horn.) Honda (Gramineae) and *Saccharum spontaneaum*, often reach heights exceeding 2–3 m and have extensive root systems that help them regenerate quickly after fire. Other common species are *Eupatorium odoratum*, *Microstegium vagans*, and *Urena lobata*.
Intermediate secondary vegetation	ISV	One-story 'forest' dominated by two bamboo species: **nua** and **giang** (*Ampelocalamus patellaris* (Gamb. Emend. Stap.) Stap. (Gramineae, Bambusoideae). Other representative species include *Alpinia blepharocalyx* K. Sch. (Zingiberaceae), *Vernicia montana* Lour. (Euphorbiaceae), *Cyperus nutans*, *Livistona saribus* (Lour.) Chev. (Palmae), *Pteris vittata* L. (Pteridaceae), and *Styrax tonkinensis* (Pierre) Pierre *ex* Guill. (Styracaceae). The understory is composed primarily of bamboo litter and shoots emerging from extensive root systems.
Forest	F	Disturbed secondary evergreen broadleaf forest, attaining heights of 25–30 m. The discontinuous upper (25–30 m) and complex secondary (8–25 m) stories include the following representative tree species: *Heteropanax fragrans* (Roxb.) Seem. (Araliaceae), *Vernicia montana*, *Alphonsea tonkinensis A. DC.* (*Annonaceae*), *Melicope pteleifolia* (Champ. *ex* Bth.) T. Hart. (Rutaceae), *Garcinia planchonii* Pierre (Guttiferae), *Ostodes paniculata* Bl. (Euphorbiaceae), *Archidendron clypearia* (Jack) Niels. ssp. *clypearia* var. *clypearia* (Leguminosae, Mimosoideae), and *Schefflera heptaphylla* (L.) Frod. (Araliaceae). A bushy understory (2–8 m) and the forest floor includes *Breynia retusa* (Denn.) Alst. (Euphorbiaceae), *Bridelia hermandii* Gagnep. (Euphorbiaceae), *Cyperus nutans*, *Dioscorea depauperata* Prain and Burk. (Dioscoreaeceae), *Rauvolfia cambodiana*, *Ficus variegata* Bl. (Moraceae), *Livistona saribus*, *Miscanthus japonicus*, *Ostodes paniculata* Bl. (Euphorbiaceae), *Phrinium capitatum* Lour. (Marantaceae), *Psychotria rubra* (Lour.) Poir. (Rubiaceae),and *Selaginella monospora* Spring (Selaginelaceae).
Consolidated Surfaces	CS	Highly compacted surface including roads, paths, and dwelling sites. Little or no vegetation exists on these frequently used surfaces.

Vegetation descriptions are based on identifications by CRES botanists (no vouchers collected); words in bold are the common Vietnamese names.

Median K_s for consolidated surfaces (7 mm h^{-1}) was exceeded frequently by I_1 during most storms (Table 6). Anywhere from 15 to 50% of the I_1 values during six of the seven largest storms exceeded median K_s on these surfaces. During the largest event (storm 1), median K_s on CS was exceeded by I_1 a total of 136 min, or about 20% of the total storm duration (Table 6). Furthermore, rainfall intensities higher than 15 mm h^{-1} were sustained for more than 90 consecutive minutes; and the I_{10_MAX}, I_{20_MAX}, I_{30_MAX}, and

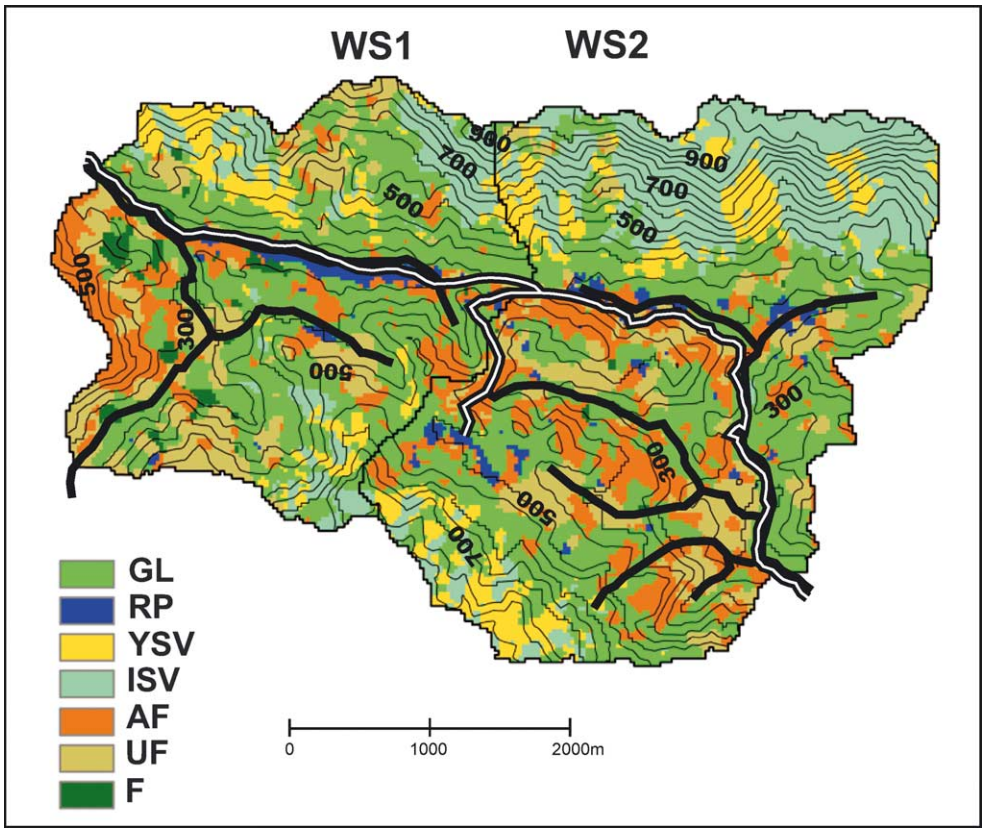

Fig. 4. Land-cover distribution in Watersheds 1 and 2; area-related statistics are given in Table 3.

I_{60_MAX} values for this storm were 85, 71, 57, and 39 mm h^{-1}, respectively. Even during the shortest storm (No. 7, 48 min), I_1 exceeded K_s on consolidated surfaces for 20 one-min periods; and the I_{30_MAX} was >25 mm h^{-1}. In contrast with the consolidated surfaces group, I_1 values rarely exceeded median K_s on GL, UF, ISV, and F land covers, i.e. fewer than 30 total 1-min periods for any one land cover for all 11 storms-providing evidence that HOF is generated infrequently on these surfaces. For the remaining two surfaces, AF and YSV, one-min periods where $I_1 > K_s$ were more common (115–210).

In Table 7, KINEROS2-predicted HOF depths for the 11 storms are shown to agree with the I_1 and K_s comparisons. The greatest HOF depths occur for consolidated surfaces. Thereafter, the following ordering applies: {AF, YSV} > {F, ISV} > {GL, UF}. Storms 10 and 11 are not sufficient in magnitude to generate HOF on any

Table 3
Area and patch-related statistics for major land covers in Tanh Minh (WS1 and WS2 combined)

Land cover	Area (ha)	Area (%)	Patches (–)	Patch area (ha)
UF	325.9	15.2	104	3.1
AF	330.3	15.4	149	2.2
GL	806.1	37.7	59	13.7
YSV	202.3	9.5	87	2.3
ISV	386.9	18.1	53	7.3
F	27.3	1.3	29	0.9
RP	59.2	2.8	50	1.2
Total or mean	2138	100	531	4.0[a]

Land covers are upland field, abandoned field, grassland, young secondary vegetation, intermediate secondary vegetation, forest, and rice paddy. *Note*. Consolidated surfaces (CS, not listed) likely comprise ≤1% of the total area.

[a] Calculated as total area/total patch number (2138 ha/531 patches).

Table 4
Descriptive statistics for K_s and bulk density for selected hillslope land covers

	UF	AF	YSV	GL	ISV	F	CS
K_s ($mm\ h^{-1}$)							
Median	103	28	32	93	67	63	7
MAD	44	10	15	29	39	31	4
Mean	112	27	41	90	65	91	11
Std. dev.	78	11	27	43	48	85	9
Minimum	23	14	10	14	9	12	2
Maximum	334	45	103	173	129	290	43
Geometric mean	88	25	34	77	45	61	7
Harmonic mean	66	24	28	59	28	42	5
Skewness	1.30	0.22	0.97	0.16	0.04	1.29	1.59
Kurtosis	1.85	−1.25	0.04	−0.27	−1.71	0.46	2.59
Count	17	11	13	11	8	15	32
ρ_b ($Mg\ m^{-3}$)							
Median	1.09	1.09	0.96	1.09	1.02	0.97	1.50
MAD	0.05	0.05	0.05	0.05	0.04	0.05	0.17

Land-cover types are upland field (UF), abandoned field (AF), young secondary vegetation (YSV), grasslands (GL), intermediate secondary vegetation (ISV), forest (F), and consolidated surfaces (CS). K_s is saturated hydraulic conductivity; MAD is the medium absolute deviation (Eq. (3)); ρ_b is bulk density.

land-cover type during computer simulations, except for CS. As partial explanation, the I_{10_MAX} values for these two storms are ≤ 16 mm h^{-1}; and K_s on the two most 'hydrologically active' non-consolidated surfaces, AF and YSV, is roughly twice as high (28–32 mm h^{-1}).

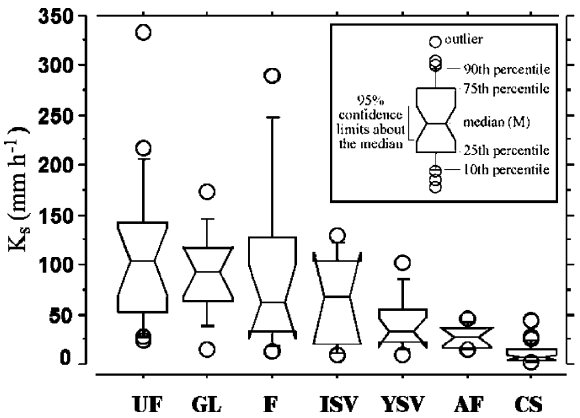

Fig. 5. Box plots of K_s for the following seven land covers: upland field (UF), grasslands (GL), forest (F), intermediate secondary vegetation (ISV), young secondary vegetation (YSV), abandoned field (AF), and consolidated surfaces (CS). Box plot features are described in the inset. Descriptive statistics are listed in Table 4.

4.4. Subsurface K_s

Fig. 7 compares box plots of surface K_s with the range of values determined at three subsurface depths (≈0.1, 0.4, and 0.7 m) for F, ISV, YSV, and UF land covers. Median values are presented in Table 8. The 0-m values are calculated from many, but not all, of the values used to calculate the medians in Table 4 (i.e. only those within a few meters of each measurement location were used). In each panel of Fig. 7, the shading highlights the data range of the forest site; and the dotted line traces the median forest values. At all depths, median K_s values for the three disturbed sites are lower than those at the forested site. Assuming the forest site has never been cultivated, the data describe the anisotropy in K_s that is present within the undisturbed soilscape, i.e. K_s decreases from about 150 mm h^{-1} at the surface to 80 mm h^{-1} at 0.4–0.7 m depth. A pronounced reduction in K_s within the soil profile is apparent at some non-forest locations. For example, surface K_s at the UF site decreases 100 mm h^{-1} to about 20 mm h^{-1} at 0.1–0.4 m depth. The low values may indicate the presence of a 'plow pan' on this surface. A similar, yet more variable, reduction of K_s with increasing depth

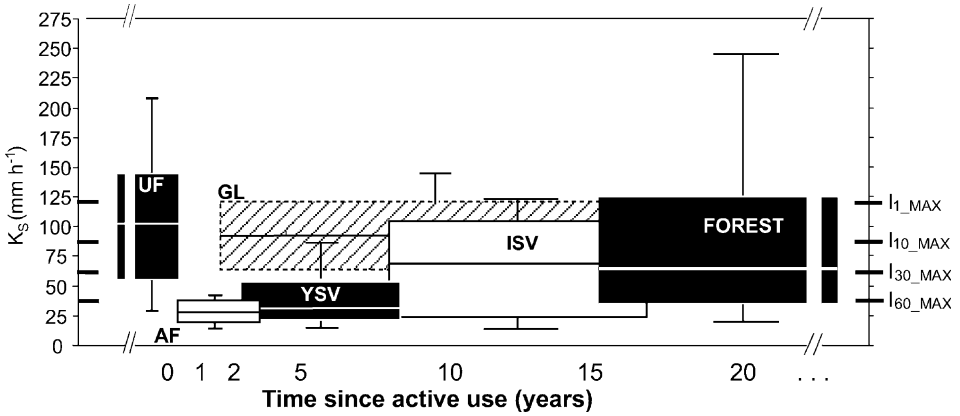

Fig. 6. Box plots of surface K_s for the following swidden-related land covers: upland field (UF), abandoned field (AF), grasslands (GL), young secondary vegetation (YSV), intermediate secondary vegetation (ISV), and forest (F). Box widths bracket the approximate age at which the land cover appears following abandonment and the age at which it gives way to a more advanced land cover. Statistical features of each box are similar to those indicated in the inset of Fig. 5. I_{1_MAX}, I_{10_MAX}, I_{30_MAX}, and I_{60_MAX} refer to maximum 1-, 10-, 30-, and 60-min rainfall intensities (from Table 5).

is noticeable at the ISV site, but strong evidence supporting a depth-related reduction in K_s is not apparent in the YSV data.

5. Discussion

5.1. Integrity of the K_s data

Of a total of 131 surface K_s measurements taken, we discarded 24 because of the following problems: (1) leaks developed where permeameter components joined; (2) good contact was not established between the permeameter base and the sand medium, causing non-uniform flow into the soil surface; (3) we discovered below the contact surface large macropores that potentially short-circuited matrix flow; or (4) we encountered difficulty in determining a realistic sorptivity (S) value from the cumulative infiltration data. The three former errors affected either water flow from the permeameter into the soil or matrix flow through the soil profile immediately

Table 5
Statistics for the eleven storm events recorded during the study period

Event[a]	Start[b] (date/time)	End (date/time)	Duration (min)	Total (mm)	I_{event}[c] (mm h^{-1})	I_{1_MAX} (mm h^{-1})	I_{10_MAX} (mm h^{-1})	I_{20_MAX} (mm h^{-1})	I_{30_MAX} (mm h^{-1})	I_{60_MAX} (mm h^{-1})
1	6/4/98, 17:21	6/5/98, 4:46	686	66.8	5.8	106.7	85.3	70.9	56.9	38.9
2	5/19/98, 9:48	5/20/98, 8:16	455	28.7	3.8	76.2	45.7	37.3	32.0	22.2
3	5/28/98, 15:03	5/28/98, 17:18	136	30.7	13.5	73.0	42.7	37.3	31.5	19.9
4	6/9/98, 16:03	6/10/98, 1:04	542	38.6	4.3	76.2	45.7	38.9	30.7	22.9
5	6/7/98, 16:06	6/7/98, 17:31	86	18.3	12.8	61.0	44.2	37.3	30.5	18.1
6	5/31/98, 16:16	5/31/98, 22:44	389	21.8	3.4	121.9	44.2	30.5	26.2	13.8
7	5/18/98, 17:15	5/18/98, 18:02	48	14.2	17.8	121.9	57.9	35.4	25.4	–
8	5/5/98, 15:22	5/5/98, 17:20	119	16.5	8.3	106.7	33.0	22.1	21.3	14.8
9	5/23/98, 23:31	5/24/98, 15:24	954	42.4	2.7	45.7	27.4	19.8	19.8	16.5
10	5/30/98, 23:24	5/31/98, 7:11	468	16.8	2.1	61.0	16.0	12.6	11.9	10.5
11	6/10/98, 20:45	6/11/98, 4:44	480	14.5	1.8	61.0	15.2	13.0	9.2	4.9

[a] Storms are ranked according to I_{30_MAX} values.
[b] Data set extends from 3/26/98 to 6/29/98; date/time format is month, day, year, hour, and minute.
[c] Values are average intensity (I_{event} = total/duration) and maximum 1-, 10-, 20-, 30-, and 60-min intensities.

Table 6
Total number of one-min rainfall values (I_1) exceeding median K_s on the specified land cover during 11 measured storms

Land cover	Storms (by rank)											Total
	1	2	3	4	5	6	7	8	9	10	11	
UF	4	0	0	0	0	2	1	1	0	0	0	8
GL	4	0	0	0	0	2	1	1	0	0	0	8
F	9	1	1	1	0	5	6	4	0	0	0	27
ISV	9	1	1	1	0	5	6	4	0	0	0	27
YSV	29	11	14	21	9	11	7	6	2	2	3	115
AF	50	19	33	31	22	16	8	8	12	3	9	211
CS	136	80	74	86	42	35	20	33	107	64	30	707

Land covers are upland field, grassland, forest, intermediate secondary vegetation, young secondary vegetation, abandoned field, and consolidated surfaces. Storms are ranked according to I_{30_MAX} values; storm statistics are shown in Table 5.

Table 7
KINEROS2 simulation of HOF (mm) generated on 30 m × 30 m plots for 11 measured storms

Land cover	Storms (by rank)											Total HOF	
	1	2	3	4	5	6	7	8	9	10	11	11 Storms (mm)	WS 1 and 2[a] (m^3)
UF	0.2	0.0	0.0	0.0	0.0	0.1	0.0	0.0	0.0	0.0	0.0	0.3	1100
GL	0.2	0.0	0.0	0.0	0.0	0.0	0.0	0.0	0.0	0.0	0.0	0.2	1800
ISV	1.4	0.1	0.2	0.2	0.0	0.1	0.2	0.1	0.0	0.0	0.0	2.3	8900
F	1.9	0.1	0.2	0.3	0.0	0.1	0.2	0.0	0.0	0.0	0.0	2.8	700
YSV	10.1	1.3	1.7	2.4	0.3	0.5	1.5	0.1	0.1	0.0	0.0	18.0	36,000
AF	13.1	2.4	2.0	3.6	0.7	2.1	2.5	0.6	0.2	0.0	0.0	27.2	89,100
CS	39.9	14.6	18.1	19.8	9.8	12.1	8.5	6.5	12.8	2.8	1.1	146.0	26,600

Land covers are upland field, grassland, intermediate secondary vegetation, forest, young secondary vegetation, abandoned field, and consolidated surfaces. Storms are ranked according to I_{30_MAX} values; storm statistics are shown in Table 5; land covers are listed in order of decreasing surface K_s (Table 4).

[a] The volumetric totals for HOF are calculated by multiplying total depth by the area each land cover occupies in both basins (Table 3); in the calculation each area is reduced proportionally to allow and estimated area value of 1% for consolidated surfaces, which are not distinguished in the land cover database.

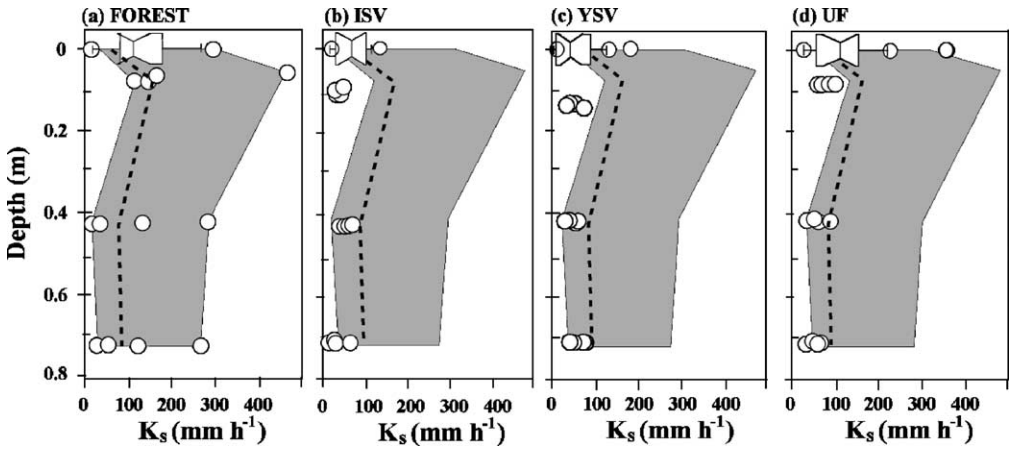

Fig. 7. Comparison of surface and subsurface K_s for four land covers (forest, intermediate secondary vegetation, young secondary vegetation, and upland field). The surface data are presented as box plots (statistical features are similar to those in Fig. 5); all subsurface values are shown. The data are summarized in Table 8. The shaded area in panels b–d corresponds to the range of values found at the forest site (panel a, the assumed control land cover); and the dotted line corresponds to the forest median value.

Table 8
Median K_s at the surface and three subsurface depths at four locations

Depth (m)	301 (UF)[a]	302 (ISV)	303 (F)	304 (YSV)
0.0	103 ± 44[b]	62 ± 37	106 ± 31	31 ± 15
0.1	22 ± 9	29 ± 6	154 ± 25	57 ± 16
0.4	17 ± 9	51 ± 11	84 ± 59	43 ± 10
0.7	43 ± 15	9 ± 3	83 ± 44	34 ± 5

[a] Numbers refer to MET station locations in Fig. 3c; corresponding land covers are upland field (UF), intermediate secondary vegetation (ISV), forest (F), and young secondary vegetation (YSV).
[b] Median values ± one MAD (Eq. (3)); $n = 4$ for each subsurface data set; $n = 17$, 7, 8, and 24 for the 0-m depth at each of the four sites, UF–YSV, respectively.

below the permeameter, thereby invalidating Eq. (1). Cleaning, resealing joints, and reassembling threaded components using joint tape can alleviate problem 1. Problems 2 and 3 were discovered during inspection of the subsurface soil following measurement. In the final problem, if the S estimate is too high, a negative value of K_s will result from Eq. (1). This is in part related to uncertainty in the Θ_0 and Θ_n values, which are determined from two separate soil samples. It also stems from difficulty in determining within the logged data precisely when the water exits the sand medium and enters the soil. In a prior work (Ziegler and Giambelluca, 1997), we use the lowest value of S in the data set when negative values were encountered. In this work, however, we discard the measurement. After eliminating potentially spurious values, some datasets were so small ($n < 10$) that it was not prudent to use standard tests to identify 'statistically indistinguishable' groups, thereby necessitating the use of a visual analysis technique. Finally, because most of our measurements come from two geographically small areas, we cannot quantify the variability that results from differences in soil type. Herein, we assume that the observed variation in K_s is produced by land cover differences.

5.2. Recovery in surface K_s

The general sequence of land-cover evolution following clearing for shifting cultivation in Tanh Minh is described by the following:

$$\mathrm{UF} \xrightarrow{2-4} \mathrm{AF} \xrightarrow{1-2} \begin{cases} \mathrm{YSV} \xrightarrow{6-10} \mathrm{ISV} \xrightarrow{8-15} \mathrm{F} \\ \mathrm{GL} \xrightarrow{?} \mathrm{F} \end{cases}$$

The numbers represent the approximate years to complete the transition from one land cover to another. After 2–4 years of cropping, fields are abandoned. In one instance, young secondary vegetation emerges within two years. This bamboo-dominated vegetation slowly matures into secondary forest within 15–25 years. Grasslands are considered to be an alternative replacement land cover, from which the timing of succession to forest we do not fully understand (discussed below).

Within the land-cover evolution, sequence a significant reduction in K_s takes place shortly after abandonment (Fig. 6). Abandoned fields, for which we measured K_s approximately 6–9 months following harvest, had the lowest median K_s values of any non-consolidated surface (28 mm h^{-1}; Table 4). Similarly, mean K_s on cultivated fields in northern Thailand dropped from 350 to 130 mm h^{-1} during the six months following abandonment (Ziegler et al., 2001; Giambelluca, 1996); and Chandler and Walter (1998) reported an analogous pattern in the Philippines. Reduction in K_s may be related, in part, to (1) consolidation during maintenance and harvesting; and/or (2) filling of surface pores by fines during the rainy season and the subsequent sealing/crusting in dry season following harvesting. During the period represented by the AF class, HOF generation may occur more frequently than during any other period of the usage/recovery sequence, except when the surface is affected by consolidation (e.g. the presence of paths). This was also the case at the Thailand site, where HOF was generated for relatively small depths of simulated rainfall on the abandoned field surface, but not on advanced fallow fields.

At Tanh Minh, the YSV develops within 1–2 years following abandonment, setting the stage for an increase in K_s that occurs gradually over the course of the next several years. With the maturation of the secondary regrowth, K_s increases toward a value represented by ISV, and eventually, that of forest. This long-term (15–25 years) recovery in K_s, depicted in Fig. 6, is likely allied

with increases in pore connectivity brought about by physiological processes, such as increased root turnover. If, however, GL becomes the initial vegetation type following abandonment, surface K_s recovers within a few years to a magnitude associated with that of the pre-swiddening era. Again, grasslands have the highest K_s values (> 90 mm h^{-1}) of any post-cultivation land cover in Tanh Minh; and GL is the largest land-cover group, occupying 38% of the total area in both watersheds (Table 3). In following, some of the prolonged risk of accelerated HOF generation in Tanh Minh is likely mitigated simply by the emergence of a grassland instead of young secondary vegetation, a land cover that occupies less than 10% of the total watershed area.

Despite the hydrological benefit of having relatively high K_s, grasslands are viewed negatively as an alternative to YSV (Appendix A). While the progression from YSV to bamboo- and tree-dominated land covers is straightforward (i.e. YSV, ISV, and F have many species in common), succession from grasslands to advanced vegetation types is unclear. Within grasslands in SE Asia in general, dominant species such as *Imperata cylindrica* tend to out-compete other vegetation—especially when fires are frequent. In the case of *Imperata*, it could remain the dominant species for an indefinite period of time until this shade-intolerant grass gives way to taller vegetation, including other weedy grassland-associated species, such as *Eupatorium* ssp. (cf. Ivens, 1983). With regard to hydrology, K_s should remain relatively high following any intermediate transition so long as the surface is not disturbed (in this respect, we did not study the influence of fire on infiltrability). Nevertheless, grasslands potentially play two important roles in mitigating some of the hydrological impacts within the fragmented landscape: (1) they initiate a faster recovery of surface K_s, thereby reducing the period of time when HOF generation is accelerated; and (2) they act as hillslope buffers, capable of infiltrating some depth of overland flow generated upslope (Ziegler et al., submitted paper). In either case, grasslands likely contribute to a reduction in hillslope surface erosion and subsequent sediment delivery to the stream.

5.3. Accelerated HOF generation in the fragmented landscape

The indices in Tables 6 and 7 demonstrate that HOF generation is more likely to occur on AF and YSV during typical storms than on the three more-advanced non-consolidated surfaces (GL, ISV, and F). Although AF and YSV occupy only a little more than 40% of the surface area as GL, ISV, and F combined, they generated an order of magnitude more HOF during 11 simulated storms ($\approx$125,000 versus 11,000 m^3, Table 7). Less rainwater infiltrates into these 'hydrologically active' surfaces, thereby producing HOF sooner in events and for more events than the other surfaces. Thus, they play the role of HOF sources on the fragmented hillslope; the other three surfaces with higher K_s, play the role of potential buffers. The grassland land cover is the most abundant potential buffer of overland flow in Tanh Minh; however, grasslands are not currently used intentionally for this purpose. Forest fragments may have a reduced role in mitigating hillslope overland flow because areal extent is small (roughly 1%; mean patch size is $\leq$1 ha); and many remnant patches are located on peaks and ridges, above the surfaces where the accelerated runoff is created (Ziegler et al., submitted paper).

5.4. Consolidated surfaces

Saturated hydraulic conductivity values are indistinguishable for the three CS surfaces (paths, dwelling sites, and roads). Path K_s ranges from 4 to 43 mm h^{-1}, with a median value of 12.6 mm h^{-1}. Dwelling sites and roads have lower median K_s: 6.2 and 6.8 mm h^{-1}, respectively. Corresponding bulk densities are 1.24, 1.47, and 1.65 Mg m^{-3}, respectively. The K_s data are similar in magnitude to those collected in northern Thailand, where path, dwelling site, and road values are also much lower than those for any other surface found typically in fragmented upland watersheds (means = 8, 24, and 15 mm h^{-1}, respectively; Ziegler et al., 2001). Although compacted surfaces often represent a small proportion of the total catchment area (estimated at $<$1% in Tanh Minh), they contribute disproportionately to storm runoff hydrographs because low K_s allows generation of HOF even during small storms when other runoff

generation mechanisms may not be activated. In addition, conveyance of CS-related overland flow to the stream channel is high, owing to connectivity with, and proximity to the stream. This is particularly true for dwelling sites, which in Tanh Minh are typically located adjacent to the stream and/or next to rice paddies. It is also true for roads, which typically drain directly into the stream. As shown in Table 7, consolidated surfaces generate approximately the same volume of basin-wide HOF as YSV during the 11 simulated events, and approximately one-third that generated on abandoned fields. These two surfaces have at least 8 and 14 times, respectively, more surface area than CS. Some caution is needed in interpreting these basin estimates because the 1% contributing area value for consolidated surfaces is estimated (see footnote in Table 7). Nevertheless, the importance here is not simply that a large volume of HOF is generated, rather, there is a high probability that most CS-related HOF will enter the stream. For example, observations of flow paths on a 3-km road section in Tanh Minh indicate that 80–90% of the road length drains directly into the stream channel or other features (e.g. ditches, channels) that are linked directly to the stream. In contrast, conveyance of AF-generated HOF to the stream is lower because of buffering by downslope land covers of higher K_s (Ziegler et al., submitted paper).

Footpaths play a role as potential source areas for HOF, that accelerates surface erosion both on the paths themselves, and importantly, on adjacent non-consolidated surfaces. Path-generated HOF can also contribute to accelerated surface erosion in upland fields, where loose soil material on the hoed surface is susceptible to detachment/entrainment by overland flow—particularly when crop cover is sparse. During storm 5, for example, we observed surface runoff on a field where we would not anticipate the generation of HOF: e.g. no I_1 values exceed the median upland field K_s value (Table 6). Field inspection after the storm revealed an access path in the immediate vicinity of where overland flow was observed. In contrast with UF, almost half the I_1 values during the 86-min storm 5 exceeded median path K_s (12.6 mm h^{-1}); note that the $I_{60\_MAX} > 18$ mm h^{-1} (Table 5). Almost 10 mm of HOF is predicted for the CS land-cover type during the KINEROS2 simulations for this 18-mm storm, but that none is predicted for the UF surface (Table 7). We observed similar path-generated HOF on uplands fields during other day-time storms as well: e.g. storms 2 and 8.

Collectively, the field observations and HOF indices demonstrate that the occurrence of path-related surface erosion on upland fields is probably a common phenomenon during medium-to-large seasonal storms. We do not recognize UF as a typical hillslope 'buffer' land cover in the sense that we recognize grasslands or forest (i.e. based solely on high K_s, Section 5.3). Rather, we view UF as a hybrid: (1) it may act as a HOF source, for example, when footpaths or other trampled areas enhance HOF generation; or (2) it may serve as a buffer, particularly if the soil surface was hoed recently, contains berms/furrows running horizontally across the slope, and is located immediately below a HOF source (Ziegler et al., submitted paper). On a scale finer than that which we are considering for this analysis, upland field surfaces can potentially infiltrate water generated on footpaths located within their boundaries if flow remains below some critical velocity/volume (a phenomenon that is related, in part, to path density).

Erosive, path-related overland flow also exists on surfaces having advanced forms of vegetation. For example, many permanent footpaths run perpendicular to the prevailing slope, ushering high-velocity flow downslope during most rain events. In the absence of switchbacks or drainage features, little opportunity exists for overland flow to enter adjacent vegetated lands of higher K_s. This is particularly the case on older trails that have incised into the hillslope. We believe that most of this type of overland flow is Hortonian, generated on the path itself or on a moderately compacted adjacent surface. Basin access paths, like field paths, therefore contribute to enhanced surface runoff and erosion throughout the rainy season.

5.5. Role of storm structure in HOF generation

Additional insights regarding the timing of HOF generation can be gleaned from the diagnostic simulations. The KINEROS2 modeling scheme takes into account the role of selected time-dependent phenomena that influence infiltration: e.g. initial relative saturation (SAT), the redistribution of water

during extended dry intervals between HOF-producing periods, and pre-wetting by initially small rainfall depths that may precede a HOF-producing period (Smith et al., 1993; Corradini et al., 1994). Obvious in the KINEROS2-simulated runoff time series is how HOF generation is influenced by storm structure (e.g. consecutive high rainfall periods or dry periods that allow recovery of soil moisture). Periods with sustained high rainfall intensity values have the propensity to generate HOF, as is apparent when comparing storms 7 and 3. On the AF land cover, for example, simulated HOF is greater during storm 7 (2.5 versus 2.0 mm, Table 7), despite storm 3 having more periods where $I_1 > K_s$ (33 versus 8, Table 6). In partial explanation, the I_{10_MAX} of storm 7 is greater than that for storm 3 (57.9 versus 42.7 mm h^{-1}, Table 5). Much of the simulated runoff during storm 7 is generated from a 6–8 min period, which is initiated by a 120 mm h^{-1} rainfall burst, followed by four 1-min periods where I_1 exceeded 75 mm h^{-1} (Fig. 8). In contrast, I_1 for storm 3 rarely exceeds 50 mm h^{-1}, and is typically less than about 30 mm h^{-1}. A smaller volume of discharge is simulated, even though storm 3 lasts 98 min longer than storm 7, has more total minutes of active HOF generation, and has more than twice the total rainfall depth (31 versus 14 mm). This example illustrates that simply knowing the number of periods when $I_1 > K_s$ is not always a reliable index of HOF generation; the temporal pattern of high/low rainfall intensity periods is important. Furthermore, the comparison shows the importance of collecting minutely rainfall data.

5.6. Conceptual model of potential changes in surface and subsurface storm flowpaths

The box plots in Fig. 7 show that each of the three disturbed sites has subsurface K_s values that are lower than those found at the forest site, which we believe represents a relatively undisturbed control. Reductions in subsurface K_s may result from changes in vegetation, which equate to changes in rooting depth, root density, and root turnover. These phenomena influence K_s by affecting total porosity and pore connectivity. The reductions may also be related to surface lowering via erosion, such that deeper, compacted soil layers with reduced K_s are now located closer to the surface. In support, Vien (1997) reported a soil loss rate on active/fallow fields in Tanh Minh of approximately 0.015 m yr^{-1}. At this rate, in only a few decades the landscape could lower the 0.2–0.4 m needed to produce the magnitude of near-surface K_s values we found on disturbed lands.

The decrease in K_s with depth below the disturbed land covers potentially retards deep infiltration of rainwater, thereby contributing to the creation of a horizontal flow component for some storms and some antecedent conditions (cf. Elsenbeer, 2001). The horizontal flow component could produce RF in areas where it would not likely occur prior to disturbance. In Fig. 9, we present conceptual models of plausible hydrologic flowpaths below some of the land-cover surfaces in the two fragmented basins.

We believe overland flow occurs infrequently on undisturbed, forested lands (Fig. 9a) in Tanh Minh where the soil is relatively deep because (1) surface K_s is high in comparison with sustained rainfall intensities; (2) the naturally occurring decrease in K_s with depth is not acute enough to create a near-surface perched water table capable of generating substantial volumes of subsurface flow during most storms (Table 8; Fig. 7); and (3) we did not observe active preferential flow mechanisms, such as piping. With respect to surface K_s, the two HOF indices in Tables 6 and 7 indicate HOF generation on the forest landcover is not substantial—and if our median K_s value for forests is low (Appendix B), HOF generation in Tanh Minh forests may be even more rare than indicated by the indices. With respect to subsurface K_s, the median forest value at about a 0.4-m depth is approximately 80 mm h^{-1} (Table 8), a magnitude that rainfall intensity rarely exceeded for sustained periods during observed storms (e.g. see the I_{10_MAX} values in Table 5). We acknowledge the potential for overland generation (HOF or otherwise) on forested slopes where rock outcrops are present, or where soil depth is shallow. Again, these physical conditions do occur in Tanh Minh because much of the remaining forest is located on rocky peaks, hollows, and steep slopes.

In contrast with the forest scenario, disturbed land covers have comparatively low values of surface and subsurface K_s (Fig. 9b and c). For example, lower surface K_s on abandoned fields (area = 15.4%) and young secondary vegetation (area = 9.5%) dictates that HOF would be generated for smaller rainfall depths, as demonstrated in the KINEROS2 simulations

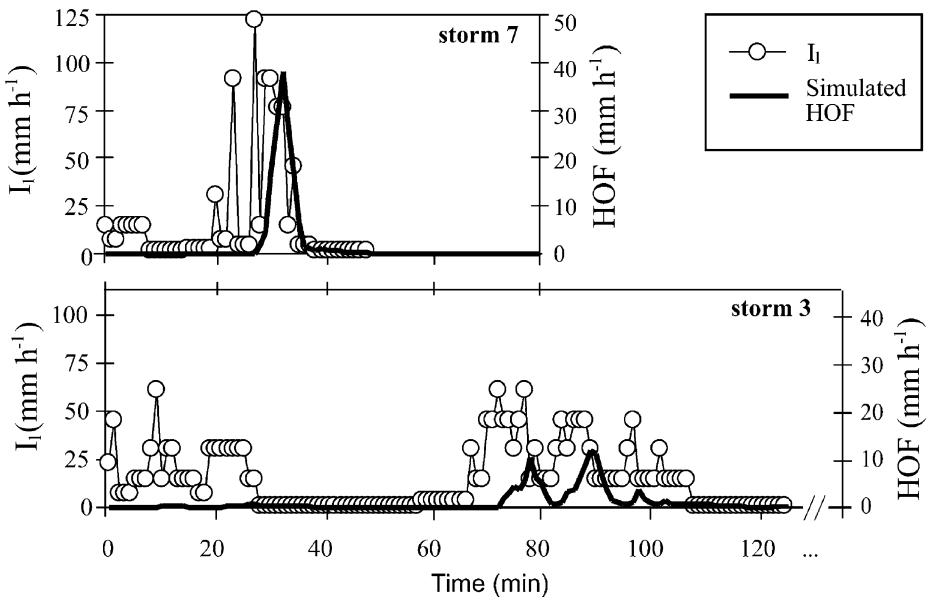

Fig. 8. Comparison of one-minute rainfall intensity (I_1) and Horton overland flow (HOF) for storms 7 and 3 (Table 5). HOF is simulated for a 30 × 30 m abandoned field at one-min time steps using the KINEROS2 runoff model.

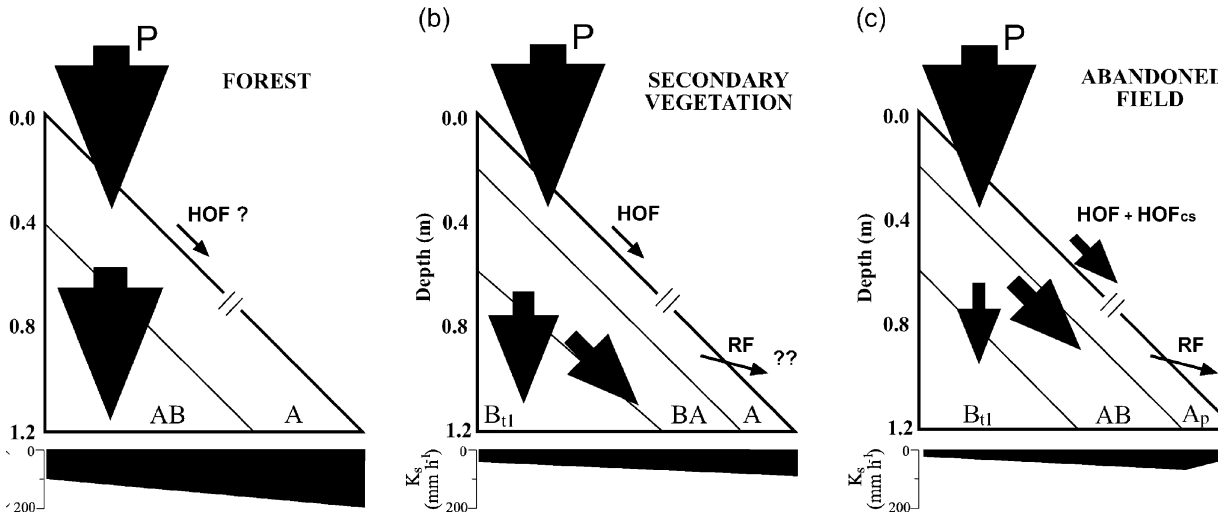

Fig. 9. Conceptual model of vertical and horizontal stormflow paths for some land covers found in Tanh Minh (in the spirit of Elsenbeer et al., 2001). Flow path magnitude and direction are inferred from measured K_s at four depths within the soil profile, including the surface. Change in K_s with depth (i.e. anisotropy) is shown in the scale at the bottom of each diagram. HOF and RF refer to Horton overland flow and return flow, respectively. The '?' signifies that HOF is probably rare for this particular land cover, but may occur in some situations (e.g. very shallow soil, rock outcrops). HOF_{cs} refers to HOF generated on consolidated surfaces, such as footpaths. The '??' signifies that the occurrence of RF is dependent, in part, on topography and storm characteristics.

(Table 7). The abandoned field scenario in Fig. 9c depicts the effect of having consolidated paths (e.g. those left over from the active-use period) contributing to enhanced HOF generation. Highlighted in Fig. 9b and c are the consequences of disruption of subsurface K_s on water movement in the soil profile. For both surface types, potential flow-restricting layers of low K_s occur at relatively shallow depths. For example, K_s values range from 30 to 60 mm h^{-1} at depths of 0.1–0.4 m. Saturated hydraulic conductivity of this magnitude is probably low enough to produce lateral flow components during storms of long duration and/or high rainfall intensity, e.g. in storm 1 the I_{30_MAX} and I_{60_MAX} values were 57 and 39 mm h^{-1}, respectively (Table 5). Whether or not the lateral components are transformed into RF on the hillslope is dependent not only on storm characteristics (including antecedent soil moisture), but on the geomorphological structure of the landscape.

6. Conclusions

Fragmentation in Tanh Minh results from a long history of human disruption. The landscape is currently a mosaic of land covers differing in infiltration characteristics, and therefore, differing in the propensity to generate overland flow. Concurrent with the succession to forested land cover, an increase in infiltrability fosters a reduction in the propensity to generate overland flow. The timing of this recovery, however, is determined in part by the initial type of vegetation that emerges. Although our data were collected within two relatively small geographical areas, and we could not account for the influence of soil heterogeneity on the variability of our K_s measurements, we believe the following specific conclusions can be drawn:

1. The fundamental activities associated with timber removal and swidden agriculture have reduced the saturated hydraulic conductivity within the near-surface soil profile. Reductions of surface K_s result in a greater likelihood of HOF generation. Reductions in subsurface K_s may increase the frequency of overland flow generated by non-Hortonian mechanisms (e.g. return flow), particularly during large seasonal storms.
2. Surface K_s on abandoned swidden fields is low compared with both the cultivated surfaces that exist before, and the more densely vegetated surfaces that follow abandonment. During the 1–2 year period following abandonment of a swidden field, the likelihood of HOF generation is the highest of any time during the swidden/fallow cycle—except when affected by consolidation (e.g. paths). Over time, various types of secondary vegetation emerge, bringing about a recovery in K_s, thereby reducing the propensity of HOF generation. The emergence of grasslands, which have the highest K_s of any measured surface, fosters a faster recovery in infiltrability than the emergence of a bamboo-dominated land cover.
3. Consolidated surfaces such as roads, footpaths, and dwelling sites contribute disproportionately to stormflow response because low K_s (median < 10 mm h^{-1}) allows HOF generation for small rainfall depths and low rainfall intensities. These human-created surfaces are ‘linked’ to the stream system, as they tend to be located near the stream or drain directly into it. Consolidated surfaces, which are inherently part of the fragmented landscape, contribute disproportionately to the associated hydrological impacts, despite occupying an estimated area of $< 1\%$.
4. Reduction of subsurface K_s provides evidence that human disturbance has altered typical subsurface hydrological pathways, thereby creating an opportunity for non-Hortonian overland flow to be generated on fragmented hillslopes. Profiles beneath human-disturbed surfaces show an enhanced reduction in K_s with depth, as compared with relatively undisturbed forested lands. If depth-related decreases in K_s are large enough to create a perched water table, a substantial lateral subsurface flow component may be produced during large storms, resulting in the generation of return flow.
5. Timber extraction and swidden agriculture have been practiced in Tanh Minh for decades, perhaps centuries. The K_s that exists at any given location is the result of a continual sequence of disruption that began long before the current land cover came into existence. The subsurface K_s patterns observed below the non-forest land covers, therefore, probably describe the range that exists below all disturbed surfaces. Over time, the root structures

associated with advanced secondary vegetation covers should act to counter reduced K_s. This recovery to a pre-disturbance magnitude would likely take much longer than the recovery of the surface K_s. Thus, the impact of land-cover conversion on overland flow generation may linger on the fragmented landscape long after the characteristics of the surface vegetation indicate otherwise. Knowledge of surface K_s alone, therefore, is not a sufficient index of the influence of human activity on overland flow generation.

Acknowledgements

This paper results from joint work conducted by researchers from the University of Hawaii, East–West Center (Honolulu, HI), and Center for Natural Resources and Environmental Studies (CRES) of the Vietnam National University, Hanoi. Financial support for the Hawaii-based team was provided by a National Science Foundation grant (no. DEB-9613613). Partial funding for the publication of this manuscript was provided by the National University Singapore grant no. R-109-000-031-112. Alan Ziegler was supported by an Environmental Protection Agency STAR fellowship. We thank the following for support during the project: Lian, Mai, and Tranh Bin Da (field work); Lan (field work, description of cropping system and landuse history of study site); Le Trong Cuc, Nghiem Phuong Tuyen, Dao Minh Truong and the other CRES staff in Hanoi; D. Plondke and S. Leisz (GIS analysis); R.A. Sutherland (analyses, chasing dead ends); and finally, the Tay villagers who welcomed us in their community. This paper benefited from critical reviews by Helmut Elsenbeer (Universität Potsdam) and Sampurno Bruijnzeel (Free University Amsterdam).

Appendix A. Grasslands in Tanh Minh

Negative connotations regarding the grassland land cover may relate to the seemingly invasive manner in which some grasses (esp. *I. cylindrica*) typically come into existence in swidden-based systems of SE Asia, and to their persistence thereafter (Potter, 1997; Schmidt-Vogt, 1999). Stands of *Imperata* often invade abandoned fields—particularly those that were burned repeatedly for agricultural preparation and weed control. Because the invaded lands are at the end of a swidden cycle, they are likely degraded (e.g. nutrients may be depleted and/or surface erosion may have removed some depth of top soil). Thus, the perceived 'invasion' may be the result of, but not the cause of, abandonment (Andrews, 1983): a classic example in SE Asia is the establishment of *Imperata* grasslands on abandoned opium fields following the removal of shade, while the grass was in seed or seedling stage (cf. Gibson, 1983). The Tay may dislike grasses such as *Imperata* because they create the burden of having to be weeded from swidden fields, and they are not a crucial resource in daily life (e.g. limited cattle grazing is practiced in Tanh Minh, and the Tay typically use *Livistona saribus* (Lour.) Chev. (Palmae) for roof thatching). Without substantial need, a negative attitude by local inhabitants toward *Imperata*—or any other invasive grass for that matter—would resemble that found commonly among other groups in SE Asia (cf. Dove, 1984).

Appendix B. Forest K_s

Although the median forest K_s value is relatively high, it is lower than what we expected to find in a forest with moderate disturbance. Again, operation of the disk permeameter requires a relatively flat measurement surface. Most forested terrain in Tanh Minh is not flat; and some forest patches are simply inaccessible. Our measurement sites therefore tend to be located on level sites where human/animal trampling may have consolidated the surface, thereby reducing K_s. In addition, more than a third of the forest measurements (5 of 13) were taken near the forest edge, where edge-versus-interior vegetation differences could also affect infiltration. However, preliminary testing (non-parametric Mann Whitney U-test) did not provide convincing evidence that edge and interior K_s values were different (median $K_s = 63$ versus 106 mm h^{-1}, respectively; Tied P-value $= 0.189$ for MW-U). If a low bias does exist for the forest data, it may also exist for other land covers

as well. For example, many of the YSV and ISV sites were also located in similarly flat areas that were possibly affected by trampling.

Comparisons with data from other tropical locations indicate that our seemingly low forest K_s values (low relative to near-subsurface K_s) may not be unusual. For example, ADZ found surface K_s (≈ 70 mm h^{-1}) in a disturbed forest in northern Thailand to be lower than that measured at a depth of 0.2 m (≈ 80 mm h^{-1}; Ziegler, 2000). There, K_s was measured with the same Vadose Zone disk permeameters herein. Similarly, Elsenbeer et al. (1999) reported surface K_s values on Latisol soils in a rainforest in Rondonia State, Brazil to be a fraction of that at a 0.15-m depth (medians are approximately 10 and 70 mm h^{-1}, respectively). In the Brazil study, the researchers speculate that a prolonged dry season in the Southern Hemisphere winter may create hydrophobicity in the forest soil. Thus, water repellency would reduce the active area of infiltration, thereby producing an underestimation of K_s by their Soil Moistures System (Tuscon, AZ) permeameter. Similarly, both the Thailand and Vietnam study sites have distinct, dry winter periods that could promote hydrophobicity. To date, hydrophobicity has not been verified conclusively at any of the three sites (H. Elsenbeer, personal communication).

References

Andrews, A.C., 1983. *Imperata cylindrica* in the highlands of northern Thailand: its productivity and status as a weed. Mountain Research and Development 3 (4), 386–388.

Bosch, J.M., Hewlett, J.D., 1982. A review of catchment experiments to determine the effect of vegetation changes on water yield and evapotranspiration. Journal of Hydrology 5, 3–23.

Brooks, R.H., Corey, A.T., 1964. Hydraulic Properties of Porous Media, Hydrology Paper 3, Colorado State University, Fort Collins, CO, 27 pp.

Bruijnzeel, L.A., 2000. Forest hydrology. In: Evans, J.C., (Ed.), The Forests Handbook, Blackwell, Oxford, (Chapter 12).

Chandler, D.G., Walter, M.F., 1998. Runoff responses among common land uses in the uplands of Matalom, Leyte, Phillippines. Transactions of the ASAE 41 (6), 1635–1641.

Close, K.R., Frasier, G., Dunn, G.H., Loftis, J.C., 1998. Tension infiltrometer contact interface evaluation by use of a potassium iodide tracer. Transactions of the American Society of Agricultural Engineers 41 (4), 955–1004.

Clothier, B.E., 2000. Infiltration. In: Smith, K.A., Mullins, C.E. (Eds.), Soil Analysis Physical Methods, second ed., Marcel Dekker, New York, 565 pp.

Cook, H.L., 1946. The infiltration approach to the calculation of surface runoff. Transactions of the American Geophysical Union 27, 726–743.

Corradini, C., Melone, F., Smith, R.E., 1994. Modeling infiltration during complex rainfall sequences. Water Resources Research 30 (10), 2777–2784.

Cuc, L.T., 1996. Swidden agriculture in Vietnam. In: Rerkasem, B., (Ed.), Montane Mainland Southeast Asia in Transition, Chiang Mai University Consortium, Chiang Mai, pp. 104–119.

Cuc, L.T., Rambo, A.T., 1999. Composite Swidden Farmers of Ban Tat: A Case Study of the Environmental and Social Conditions in a Tay Ethnic Minority Community in Hoa Binh Province, Vietnam, Research Report 1, Center for Natural Resources and Environmental Studies (CRES), Vietnam National University, Hanoi, 191 pp.

Do Van, S., 1994. Shifting Cultivation in Vietnam: its Social, Economic, and Environmental Values Relative to Alternative Land Use, IIED Forestry and Land Use Series No. 3, International Institute for Environment and Development, London.

Dove, M.R., 1984. Government Versus Peasant Beliefs Concerning Imperata and Eupatorium: A Structural Analysis of Knowledge, Myth, and Agricultural Ecology. Environment and Policy Institute, East–West Center, Honolulu, HI.

Dunne, T., Black, R.D., 1970. Partial area contributions to storm runoff in a small New England watershed. Water Resources Research 6, 1296–1311.

Dunne, T., Leopold, L.B., 1978. Water in Environmental Planning. Freeman, San Francisco, CA, 818 pp.

Elsenbeer, H., 2001. Hydrologic flowpaths in tropical rainforest soilscapes: a review. Hydrological Processes 15, 1751–1759.

Elsenbeer, H., Lack, A., 1996. Hydrological pathways and water chemistry in Amazonian rain forests. In: Anderson, M.G., Brooks, S.M. (Eds.), Advances in Hillslope Processes, Wiley, New York, pp. 939–959.

Elsenbeer, H., Cassel, D.K., Castro, J., 1992. Spatial analysis of soil hydraulic conductivity in a tropical rain forest catchment. Water Resources Research 28 (12), 3201–3214.

Elsenbeer, H., Newton, B.E., Dunne, T., de Moraes, J.M., 1999. Soil hydraulic conductivities of latosols under pasture, forest and teak in Rondonia, Brazil. Hydrological Processes 13, 1417–1422.

Fox, J., Truong, D.M., Rambo, A.T., Tuyen, N.P., Cuc, L.T., Leisz, S., 2000. Shifting cultivation: a new old paradigm for managing tropical forests. BioScience 50 (6), 521–528.

Fox, J., Leisz, S., Truong, D.M., Rambo, A.T., Tuyen, N.P., Cuc, L.T., 2001. Shifting cultivation without deforestation: a case study in the mountains of northwestern Vietnam. In: Millington, A.C., Walsh, S.J., Osborne, P.E. (Eds.), Applications of GIS and Remote Sensing in Biogeography and Ecology, Kluwer, Boston, pp. 289–307.

Giambelluca, T.W., 1996. Tropical land cover change: characterizing the post-forest land surface. In: Giambelluca, T.W., Henderson-Sellers, A. (Eds.), Climate Change: Developing Southern Hemisphere Perspectives, Wiley, New York, pp. 293–318.

Giambelluca, T.W., Ziegler, A.D., Nullet, M.A., Dao, T.M., Tran, L.T., 2003. Transpiration in a small tropical forest patch. Agriculture and Forest Meteorology 117, 1–22.

Gibson, T., 1983. Toward a stable low-input highland agricultural system: Ley farming in *Imperata* cylindrical grasslands of northern Thailand. Mountain Research and Development 3 (4), 378–385.

Hewlett, J.D., Hibbert, A.R., 1967. Factors affecting the response of small watersheds to precipitation in humid areas. In: Sopper, W.E., Lull, W.H. (Eds.), International Symposium on Forest Hydrology, Pergamon Press, Tarrytown, NY, pp. 275–290.

Hibbert, A.R., 1967. Forest treatment effects on water yield. In: Sopper, W.E., Lull, H.W. (Eds.), Forest Hydrology, Pergamon Press, Oxford, pp. 527–543.

Hillel, D., 1971. Soil and Water: Physical Principles and Processes. Academic Press, New York, 299 pp.

Horton, R.E., 1933. The role of infiltration in the hydrologic cycle. Eos Transactions AGU 14, 446–460.

Hudson, N.W., 1971. Soil Conservation. Batsford, London.

Ivens, G.W., 1983. The natural control of *Imperata cylindrica* in Nigeria and northern Thailand. Mountain Research and Development 3 (4), 372–377.

Jones, J.A.A., 1997. Inadvertent impacts on hydrological processes. 1. Water quality, Global Hydrology: Processes, Resources and Environmental Management, Addison-Wesley/Longman, Essex, pp. 211–240 (Chapter 7).

Kirkby, M.J., 1988. Hillslope runoff processes and models. Journal of Hydrology 100, 315–339.

McGill, R., Tukey, J.W., Larsen, W.A., 1978. Variations of box plots. American Statistician 32 (1), 12–16.

Nguyen, D.K., van der Poel, P., 1993. Land Use in the Song Da Watershed (Northwest Vietnam), SFDP Baseline Study no. 2, Vietnamese-German Technical Cooperation Social Forestry Development Project (SFDP) Song Da, Hanoi.

Nielsen, D.R., Biggar, J.H., Erh, K.T., 1973. Spatial variability of field-measured soil-water properties. Hilgardia 42 (7), 215–259.

Parlange, J.-Y., Lisle, I., Braddock, R.D., Smith, R.E., 1982. The three-parameter infiltration equation. Soil Science 133 (6), 337–341.

Perroux, K.M., White, I., 1988. Designs for disc permeameters. Soil Science Society of America Journal 52, 1205–1215.

Potter, L.M., 1997. The dynamics of Imperata: historical overview and current farmer perspectives, with special reference to South Kalimantan, Indonesia. Agroforestry Systems 36, 31–51.

Rambo, A.T., 1996. The composite swiddening agroecosystem of the Tay ethnic minority of the northerwestern mountain of Vietnam. In: Rerkasem, B., (Ed.), Montane Mainland Southeast Asia in Transition, Chiang Mai University Consortium, Chiang Mai, pp. 69–89.

Rogowski, A.S., 1972. Watershed physics: Soil variability criteria. Water Resources Research 8 (4), 1015–1023.

Schmidt-Vogt, D., 1999. Swidden Farming and Fallow Vegetation in Northern Thailand, Geoecological Research, vol. 8. Franz Steiner Verland, Stuttgart, 342 pp.

Sharma, P.N., 1992. Status and needs for forest watershed management in Vietnam. Transactions of the American Society of Agricultural Engineers 8 (4), 461–469.

Smith, R.E., Corradini, C., Melone, F., 1993. Modeling infiltration for multistorm runoff events. Water Resources Research 29 (1), 133–144.

Smith, R.E., Goodrich, D.C., Quinton, J.N., 1995. Dynamic, distributed simulation of watershed erosion: the KINEROS2 and EUROSEM models. Journal of Soil and Water Conservation 50 (5), 517–520.

Smith, R.E., Goodrich, D.C., Unkrich, C., 1999. Simulation of selected events on the Catsop catchment by KINEROS2: a report for the GCTE conference on catchment scale erosion models. Catena 37, 457–475.

Thai, P., Nguyen, T.S., 1992. Management of sloping lands for sustainable agriculture in Vietnam. In: Sajjapongse, A., (Ed.), Technical Report on the Management of Sloping Lands for Sustainable Agriculture in Asia, Phase I, 1988–1991, Network Document no. 2, International Board for Soil Research and Management (IBSCRAM)/ASIALAND, pp. 255–320.

Tuan, V.V., 1993. Evaluation of the Impact of Deforestation to Inflow Regime of the Hoa Binh Reservoir in Vietnam, Hydrology of Warm Humid Regions, Proceedings of the Yokahama Symposium, July 1993. IAHS Publication 216, pp. 135–138.

Tukey, J.W., 1977. Exploratory Data Analysis. Addison-Wesley, Reading, MA.

USDA, 1993. Examination and Description of Soils, Soil Survey Manual, Handbook 18, United States Department of Agriculture, US Printing Office, Washington, DC, 437 pp (Chapter 3).

Van Bo, N., Phien, T., Tu Siem, N., 2001. Response to Land Degradation. In: Bridges, E.M., Hannam, I., Oldeman, L.R., Penning de Vries, F., Scherr, S.J., Sombatpanit, S. (Eds.), Oxford & IBH, New Delhi, pp. 100.

Vien, T.D., 1997. Soil erosion and nutrient balance in swidden fields of the Da Bac District, Vietnam, Final Report No. 10667, East–West Center Program on Environment, Honolulu, Hawaii, 29 pp.

White, I., 1988. Measurement of soil physical properties in the field. In: Steffen, E.L., Denmead, O.T. (Eds.), Flow and Transport in the Natural Environment: Advances and Applications, Springer, Heidelberg, pp. 59–85.

Wischmeier, W.H., Smith, D.D., 1978. Predicting Rainfall Erosion Losses, Agriculture Handbook no. 53, USDA, Washington, DC.

Zavslavski, D., Rogowski, A.S., 1969. Hydrologic and morphologic implications of anisotropy and infiltration in soil profile development. Soil Science Society of America Proceedings 33, 594–599.

Ziegler, A.D., 2000. Toward modeling road erosion in northern Thailand. PhD Dissertation. Geography Department, University of Hawaii, Honolulu, HI, USA, 105 pp.

Ziegler, A.D., Giambelluca, T.W., 1997. Importance of rural roads as source areas for runoff in mountainous areas of northern Thailand. Journal of Hydrology 196 (1/4), 204–229.

Ziegler, A.D., Sutherland, R.A., Giambelluca, T.W., 2000. Runoff generation and sediment transport on unpaved roads, paths, and agricultural land surfaces in northern Thailand. Earth Surface Processes and Landforms 25 (5), 519–534.

Ziegler, A.D., Sutherland, R.A., Giambelluca, T.W., 2001. Acceleration of Horton overland flow and erosion by footpaths in an agricultural watershed in Northern Thailand. Geomorphology 41 (4), 249–262.